Linking Carbonate Facies to Stylolite Distribution of Middle Jurassic Limestone, Onshore Abu Dhabi Oil Field

Mochammad Prahastomi[1], Sadoon Morad[2] Aisha Al Suwaidi[3] Mohammed Ali[4] Budi Muljana[5] Ryandi Adlan[6]

[1]Geology Department, Universitas Pembangunan Nasional Veteran Yogyakarta, Special Region of Yogyakarta, Indonesia

[2,3,4]Earth Science Department, Khalifa University of Science and Technology, Abu Dhabi, United Arab Emirates

[5]Geological Engineering Department, Universitas Padjadjaran, West Java, Indonesia

[6]Center of Geological Survey, Geological Agency, Ministry of Energy and Mineral Resources, West Java, Indonesia

Email: [1]moch.prahastomi@upnyk.ac.id, [2]sadoon.morad@ku.ac.ae, [3]aisha.alsuwaidi@ku.ac.ae, [4]mohammed.ali@ku.ac.ae, [5]budi.muljana@unpad.ac.id, [6]ryandi.adlan@esdm.go.id

Received: 2025-08-25 Received in revised from 2025-09-03 Accepted: 2025-09-10

Abstract

This study examines the relationship between facies and stylolitization in the Upper Araej Member carbonates of onshore Abu Dhabi. Analysis of core and thin sections identified four facies: wispy-laminated skeletal wackestone (F-1), peloidal skeletal mud-dominated packstone (F-2), coated-grain skeletal grainstone (F-3), and peloidal skeletal floatstone (F-4), deposited across a shallow carbonate ramp. Stylolites were described and measured for vertical offset amplitude to assess facies dependence. Results show facies-related tendencies in stylolite amplitude and morphology. Mud-supported facies (especially floatstones and wackestones) tend to display higher variability, with floatstones reaching amplitudes of up to 20 mm, whereas grainstones may also contain isolated high-amplitude stylolites (up to 14 mm). Packstones and wackestones, by contrast, rarely exceed 10-13 mm. Boxplots highlight greater variability in mud-rich facies, whereas grainstones exhibit narrower distributions. Statistical testing (ANOVA, $p = 0.109$; Kruskal–Wallis, $H = 3.38$, $p = 0.34$) indicates no statistically significant differences in mean stylolite amplitude across facies, although descriptive data reveal trends in variability and extremity. Jagged stylolites occur in both mud-rich and grain-supported facies, whereas wispy seams are strongly associated with micrite-rich facies and are largely absent in grainstones. Stylolites in these carbonates may act as both vertical barriers and localized porosity enhancers. Their facies-associated occurrence emphasizes the need to integrate stylolitization into reservoir models to better predict connectivity, compartmentalization, and flow behavior in Middle Jurassic carbonates.

Keywords: *Carbonate Facies; Middle Jurassic Limestone; Onshore Abu Dhabi; Stylolite; Upper Araej Member.*

1. Introduction

Carbonate rocks constitute more than half of the world's hydrocarbon reserves [1] [2] and form significant aquifers [3] [4] and CO_2 storage sites [5] [6] [7]. Their reservoir quality, however, is not solely a product of depositional fabric but is strongly influenced by post-depositional diagenetic processes. The interplay between depositional facies and diagenetic overprint generates a highly complex and spatially heterogeneous porosity-permeability system that cannot be predicted from depositional textures alone [8]-[12]. Among these diagenesis process, cementation, dissolution, dolomitization, and pressure solution play crucial roles in modifying primary porosity and permeability. Moreover, pressure-solution processes are responsible for the generation of stylolites, which are among the most common diagenetic features in carbonate successions [13]-[16]. Understanding the distribution

and development of stylolites is therefore critical to evaluating reservoir heterogeneity and performance in carbonate systems.

Stylolites are serrated dissolution seams formed through stress-induced pressure solution, where insoluble residues such as clays and organic matter accumulate along irregular solution surfaces [17]. They typically form perpendicular to the maximum stress direction and are easily recognized by their characteristic jagged morphology. Stylolites may have a dual impact on reservoir properties. On one hand, stylolites can form barriers or baffles to vertical fluid flow due to their concentration of insoluble material, thereby reducing permeability (e.g. [10] and [15]). On the other hand, they may enhance porosity locally through dissolution and leaching of carbonate minerals adjacent to the stylolite seam [18]. This duality highlights their importance in reservoir characterization, where stylolitization can either impede or facilitate hydrocarbon production depending on facies context and spatial continuity.

Considerable research has been devoted to stylolite morphology, classification, and scaling relationships. Early classifications by [17] and refinements by [20] provided frameworks for categorizing stylolite shapes and roughness patterns. Other studies have examined the role of burial depth and stress conditions in controlling stylolite amplitude and spacing, as well as their implications for fluid flow and mechanical stratigraphy [20]. Much of this work has been carried out in European carbonate systems (e.g. [20], [21]) and to some extent in the Middle East (e.g., [13]-[16]). However, despite this body of literature, relatively few studies have quantitatively examined facies-dependent stylolitization patterns within Arabian Plate carbonates, especially the Middle Jurassic Carbonate. In particular, systematic analyses linking stylolite frequency and amplitude to specific facies types in platform carbonates remain limited.

This study aims to address this gap by quantifying stylolite occurrence across different carbonate facies, including mud-rich facies and grain-supported facies. By analyzing stylolite frequency and amplitude distributions in relation to depositional facies, this work aims to identify facies-dependent trends in stylolitization intensity. The findings will provide insights into how depositional fabric and diagenetic processes interact to influence stylolite development. Furthermore, the potential implications for reservoir quality, particularly permeability anisotropy, compartmentalization, and fluid-flow behaviour will be discussed. Ultimately, this study contributes to a better understanding of stylolite-related heterogeneity in Upper Araej Member and may provide a predictive framework for evaluating similar carbonate reservoirs across the Arabian Plate.

Geological Settings

The United Arab Emirates (UAE) lies on the eastern margin of the Arabian Plate, bounded by the Qatar–South Fars Arch to the west and the Oman foreland fold-and-thrust belt to the east [20]. The region is dominated by shallow-marine epeiric carbonates interbedded with minor evaporites and siliciclastics, reflecting repeated transgressions and regressions throughout the Phanerozoic. The tectonostratigraphic evolution of the UAE is marked by three major events: (1) pre-ophiolite rifting, (2) emplacement of the Semail Ophiolite, and (3) the Zagros Orogeny [23] [24]. The rifting history, associated with the opening of the Neo-Tethys Ocean, occurred in two main phases: the late Permian and from the Early Jurassic to Late Cretaceous. These extensional phases generated widespread shallow-marine carbonate platforms across the Arabian microcontinent under relatively stable conditions. Stability ended in the Late Cretaceous with emplacement of the SW-directed Semail Ophiolite. Obduction placed ophiolitic nappes above the pre-Cenomanian passive-margin carbonates, causing flexural loading, thrusting, and folding [23]. Despite this, most of the Mesozoic carbonate shelf remained undeformed, apart from minor faulting [24] [25]. Peripheral bulge development induced uplift and erosion, particularly along the Lekhwair High and Sharjah. Sedimentation during this period shifted to deep-marine mudstones in the Upper Cretaceous, overlain by shallow-marine carbonates of the Simsima Formation [23].

The subsequent compressional phase, the Zagros Orogeny, occurred during the Late Eocene to Miocene and is linked to collision between the Arabian and Eurasian plates following closure of the Neo-Tethys [26]. Some studies, however, place initial collision in the Late Eocene–Oligocene [27] [28].

This event reactivated deep-seated faults in the frontal thrust belt and triggered uplift along the northern Oman Mountains, leading to erosion of pre-Eocene carbonates [24] [25].

The study concentrates on the Araej Formation which comprises mainly of ooid-peloidal grainstones, foraminiferal packstones, wackestones, and argillaceous lime mudstones. The study based on Ammonite content suggested the age of this formation from Bathonian to Callovian [29]. However, [30] suggested a slightly older age, which is Bajocian to Callovian (Offshore Abu Dhabi) and supported by the work of [31] which suggest a late Bajocian to Callovian (Onshore Abu Dhabi). Additionally, its equivalent formation is upper and middle Dhruma in Saudi Arabia. The Upper Araej Member made up of argillaceous mudstones which grade upwards to cemented bioclastic, ooid-peloidal packstones and foraminiferal grainstones with minor wackestone units [30]. Benthic foraminifera, *Trocholina sp.*, were found pervasively in grain dominated limestone units. The depositional facies and textural pattern of Lower Araej and Upper Araej members are relatively similar to each other. However, a study conducted by [30] suggested that in terms of diagenesis, dolomitization occurred more frequent in Upper Araej (especially in topmost part) than in Lower Araej Member. Pyrite and anhydrite replacement were reported to be present as well. A study based on onshore well Abu Dhabi reported that the topmost of Upper Araej Member made up of dolomitic packstones which coincide with residual oil and oil stain [31].

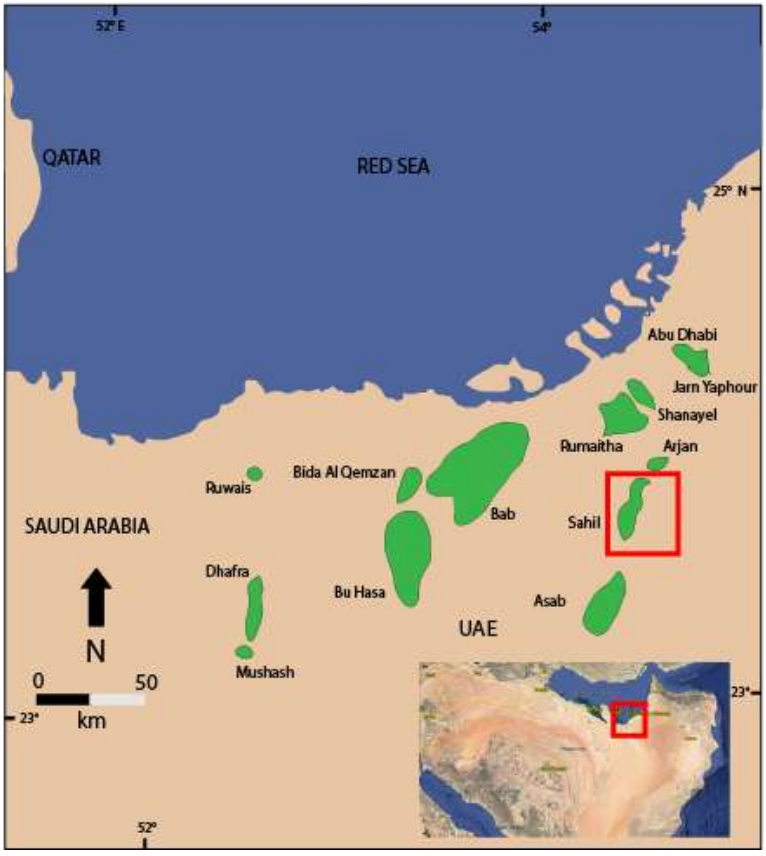

Figure 1. Research location (Modified from [32])

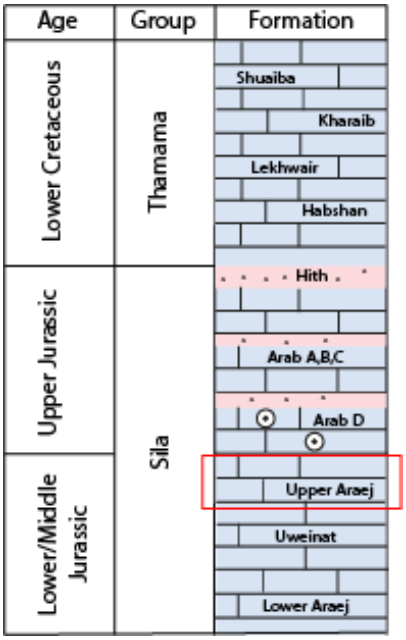

Figure 2. Stratigraphic column of Upper Araej Member [33]

2. Method

This study focuses on the Upper Araej Member (Middle Jurassic) from an oil well located onshore Abu Dhabi (Figure 1). The well is situated on the flank of an anticline. Data and interpretation presented were derived from the investigation of 36 core boxes totalling 90 feet. The carbonate classification applied in this study follows [34]. However, for analytical and practical purposes, Packstone facies are further categorized using [35] terminology as Mud-Dominated Packstone (MDP) and Grain-dominated Packstone (GDP).

The petrographic analyses of 63 half-stained thin sections were performed to characterize rock textures, grain types, lime mud percentages, calcite-dolomite percentages, mineral types, fracture, and also stylolite morphology. The depositional environment of each microfacies was interpreted based on the thin section and core description.

To evaluate the relationship between carbonate facies and stylolite development, a statistical analysis of stylolite amplitude was carried out on data collected from Floatstone, Wackestone, Packstone, and Grainstone facies in the onshore Abu Dhabi oil field. Stylolite amplitude values (in millimeters) were compiled for each facies from thin-section and core descriptions, and grouped according to petrographic classification. This work focuses on the measurement of vertical offset, a critical indicator of pressure-solution processes in carbonate rocks. The offset values, illustrated in Figure 3, are used to evaluate the relative magnitude of stylolitization and to link these features with facies-dependent patterns.

For each facies, basic descriptive statistics for the styolite were computed, including:

- Mean amplitude (mm): arithmetic average, representing the central tendency of stylolite size.
- Median (mm): the 50th percentile, used to account for potential skewness in distributions.
- Standard deviation and variance: measures of variability around the mean.
- Minimum and maximum values (mm**):** identifying the observed range of stylolite amplitudes.

- Sample count (n): indicating the number of stylolite measurements per facies.

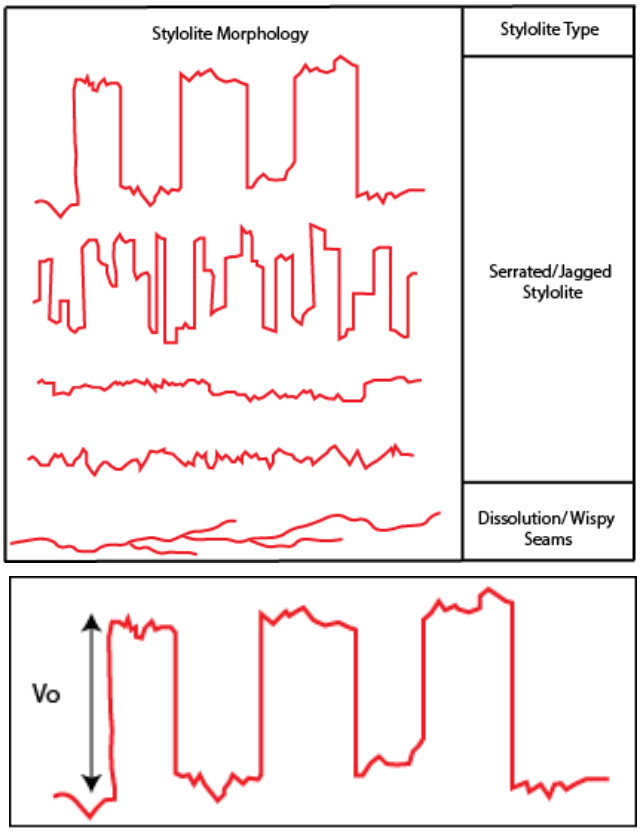

Figure 3. Stylolite type and morphology modified from [17]. The measurement of stylolte amplitude is indicated by the vertical offset (Vo).

The amplitude data were visualized using boxplots to highlight distributional properties across facies. In these plots, the lower and upper box boundaries represent the 25th percentile (Q1) and 75th percentile (Q3), the line within the box marks the median, and whiskers extend to the minimum and maximum within 1.5 × IQR. Data points outside this range were considered outliers.

To test for statistically significant differences in stylolite amplitude between facies, one complementary approach was applied: One-way ANOVA, a parametric test comparing mean amplitudes across facies. One-way ANOVA is used to test whether the means of more than two groups are significantly different. The test compares between-group variance (variation of group means relative to the overall mean) with within-group variance (variation of values within each group). The computed F-value is compared against the critical value of the F-distribution at a chosen significance level (α) to determine whether the group means differ significantly [35].

The total variation in the data is partitioned as:

$$SS\_Total = SS_{Between} + SS_{Within} \quad (1)$$

Between-group sum of squares:

$$SS_{Between} = \Sigma\ (n_i * (\bar{X}_i - \bar{X})^2),\ I = 1,\ldots,k \quad (2)$$

Within-group sum of squares:

$$SS_{Within} = \Sigma \Sigma (X_{ij} - \bar{X}_i)^2 , j = 1,\ldots, n\_i ; i = 1,\ldots,k \quad (3)$$

where:
k = number of groups (facies)
n_i = number of samples in group i
$\bar{X}_i$ = mean of group i
$\bar{X}$ = overall mean
X_{ij} = observation in group i

The mean squares (MS) are defined as:

$$MS_{Between} = SS_{Between} / (k-1) \quad (4)$$

$$MS_{Within} = SS_{Within} / (N-k) \quad (5)$$

The F-ratio is then calculated as:

$$F = MS_{Between} / MS_{Within} \quad (6)$$

where N is the total number of observations.

The Kruskal–Wallis H test was employed to evaluate whether the mean stylolite amplitude differs significantly among the four carbonate facies (Floatstone, Wackestone, Packstone, and Grainstone). This non-parametric test is an extension of the Mann–Whitney U test to more than two independent groups. It is particularly well suited to geological and petrographic data, which often violate the assumptions of parametric tests due to skewed distributions, unequal variances, and the presence of outliers. The Kruskal–Wallis test operates by ranking all observations from all groups together, then assessing whether the sum of ranks differs more than expected under the null hypothesis [37]. The null hypothesis (H_0) states that the distribution of stylolite amplitude is identical across all facies. The alternative hypothesis (H_1) is that at least one facies differs in distribution.

The test statistic is calculated as:

$$H = [12 / (N(N+1))] * \Sigma (Ri^2 / ni) - 3(N+1) \quad (7)$$

where:
k = number of groups (four facies)
N = total number of observations across all groups
ni = number of observations in group i
Ri = sum of the ranks for group i

The statistic H is approximately chi-square distributed with (k – 1) degrees of freedom, provided that each group contains at least five observations. The corresponding p-value is used to determine statistical significance at the chosen threshold ($\alpha = 0.05$). If $p < \alpha$, the null hypothesis is rejected, indicating that at least one facies differs in mean stylolite amplitude distribution.

3. Results and Discussion

3.1 Facies Characteristics and Depositional Environment

Based on optical petrographic analysis and core logging description, the studied interval was divided into four facies. The shallowing upward sequences were observed which comprises mud-dominated limestone units deposited on the subtidal open marine and grading upward into coarse grain-dominated limestone units deposited on the shoal setting. Several high frequency cycles were recorded in the succession.

Wispy-laminated Skeletal Wackestone (F-1)

This facies, developed predominantly in the basal to middle portions of the Upper Araej, is typified by pervasive wispy lamination. Contacts with the overlying packstones are most commonly stylolitic. Bioclasts are dominated by planktonic foraminifera, sponge spicules, and gastropods, with subordinate benthic foraminifera and echinoderm fragments (Figure 5a). Non-skeletal components consist chiefly of peloids. The high lime-mud content indicates deposition below the fair-weather wave base in a low-energy environment. The frequent occurrence of planktonic foraminifera is consistent with deposition in a relatively deeper, subtidal setting. The absence of restricted-lagoonal indicators (e.g., dasycladacean algae) implies open-marine circulation. Consequently, this facies is interpreted as having accumulated in a low-energy, open-platform environment, within the middle to outer ramp.

Peloidal Skeletal Mud-dominated Packstone (F-2)

Mud-dominated packstones (0.3–2.8 ft thick) are among the most widespread lithologies in the studied succession. They are typically bioturbated and stylolitized, with gradational transitions into overlying wackestones. In the middle interval, they are interbedded with massive grainstones and wackestones, whereas in the upper interval they alternate with floatstones and grainstones. The allochem assemblage is dominated by peloids and large benthic foraminifera (*Trocholina* sp.), with additional contributions from echinoderms, gastropods, and bivalves (Figure 5b). Bioturbation indicates deposition under shallow-marine conditions with relatively low sedimentation rates. The absence of miliolids and dasycladacean algae, together with the relatively high faunal diversity, supports interpretation in terms of an open-marine setting. This facies is therefore considered to represent subtidal sedimentation on an open platform, most likely within the upper to middle ramp.

Coated-grain Skeletal Grainstone (F-3)

Grainstones are concentrated in the upper part of the studied succession, where they are typically overlain by wackestones or packstones. Bed thickness varies between 0.2 and 2.6 ft. In the upper interval, grainstones occur as relatively thick and laterally continuous beds, whereas in the middle interval they are restricted to thinner and less continuous horizons. The assemblage is dominated by benthic foraminifera (*Trocholina* sp.) (Figure 5c), accompanied by bivalves, echinoderms, and gastropods, with only rare ooids. Stylolites are generally absent, but when present are jagged to rectangular and filled with cement. The absence of lime mud and bioturbation suggests deposition under high-energy conditions, likely within a shoal or beach–barrier island complex. Such hydrodynamic regimes are unfavorable for the preservation of bioturbation structures owing to persistent wave and current activity. Thin interbedded grainstones in the middle interval, however, may represent spillover lobes or low-amplitude sandwaves within a lagoonal, shallow-subtidal setting.

Peloidal Skeletal Floatstone (F-4)

Floatstones occur predominantly in the upper interval, where they are interbedded with grainstones and packstones, and less commonly in the basal interval, where they alternate with wackestones and packstones. Bed thickness ranges from 0.1 to 2.4 ft. This microfacies is characterized by a substantial lime-mud matrix. Allochems consist mainly of peloids, large bivalves, benthic foraminifera (*Trocholina* sp.), echinoderms, and gastropods, with minor bryozoans (Figure 5d). The high taxonomic diversity of the faunal assemblage suggests deposition under open-marine conditions. The abundance of peloids is consistent with a shallow-subtidal setting, while partially fragmented bivalves indicate episodic reworking by waves or currents. This facies is therefore interpreted to reflect deposition in an open-platform, shallow-subtidal environment, on the upper to middle ramp, in association with a beach–barrier island complex.

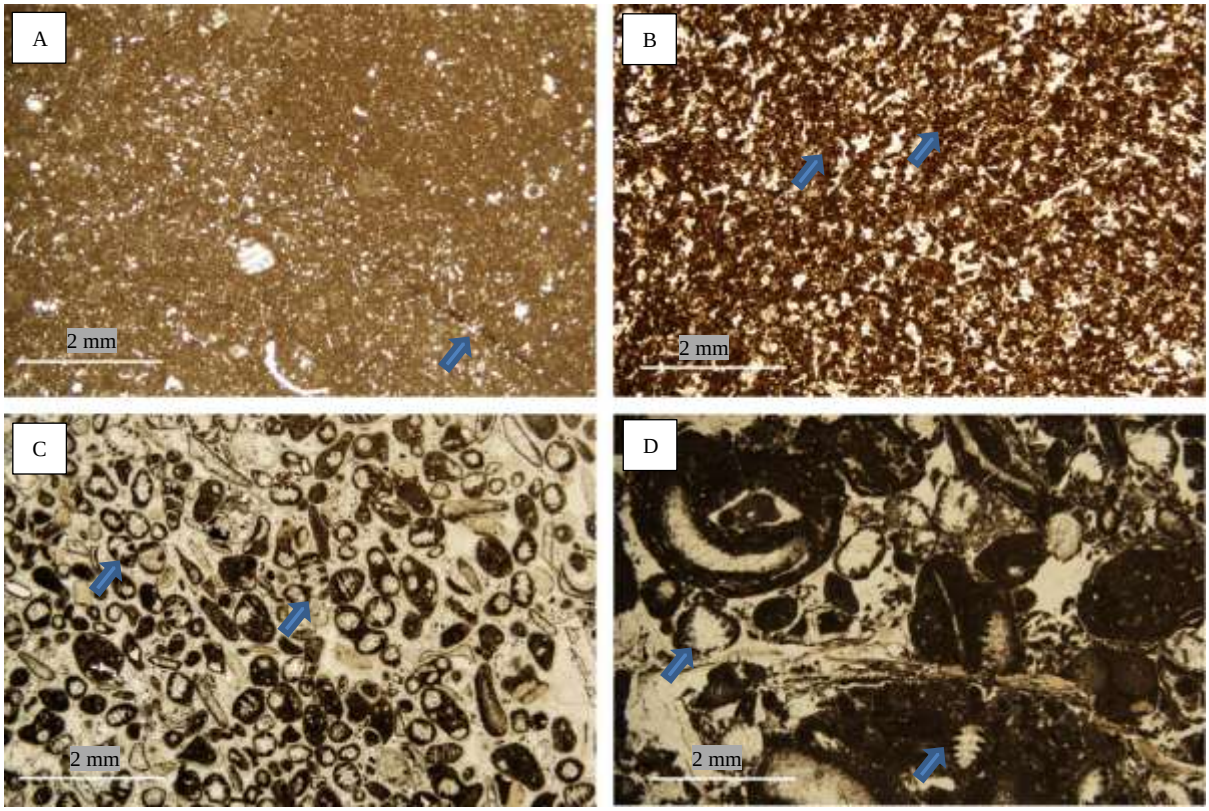

Figure 5. Optical photomicrograph in ppl showing 4 different facies in Upper Araej Member. (a) Wispy laminated skeletal wackestone, note the subtle appearance of low amplitude stylolite/wispy seams shown in blue arrow which is typically found in this facies (b) Peloidal-skeletal mud-dominated packstone facies, in this facies peloids are abundant (blue arrow). (c) Coated grain-skeletal grainstone with abundant benthic forams (Trocholina sp.) shown in blue arrow, micrite envelopes are common (d) Peloidal skeletal floatstone, the occurrence of peloid, extraclast, benthic forams (blue arrow) are significant with much larger size.

3.2 Stylolite

Two types of stylolites are recognized in the studied limestones, which are jagged/rectangular stylolite and wispy seams. Stylolites have amplitude of millimetre to centimeters and are more common in packstones, wackestones, floatstone than in grainstone. Stylolites are pervasive in the middle part of the studied interval (Figure 6a). Stylolites occurred throughout the studied interval where those with higher amplitudes (>1 cm) are encountered in the upper interval. Stylolites with low to medium amplitude (0.3 – 1 cm) are common throughout the section particularly in the upper and middle interval. Wispy seams were observed mostly in the middle and lower interval.

Jagged/rectangular stylolites (Figure 7a and 7b), which are characterized by varied amplitudes (up to 20 mm) are encountered mainly in packstones and wackestones and more rarely in grainstone. Wispy seams (Figure 7c) which are characterized by multiple anastomosing surfaces of low relief with relatively thick dark materials are encountered mainly in packstone and wackestone, and rarely in floatstone. Wispy seams in the Upper Araej Member are frequently filled with thick clay laminae, for example shown in Figure 7c.

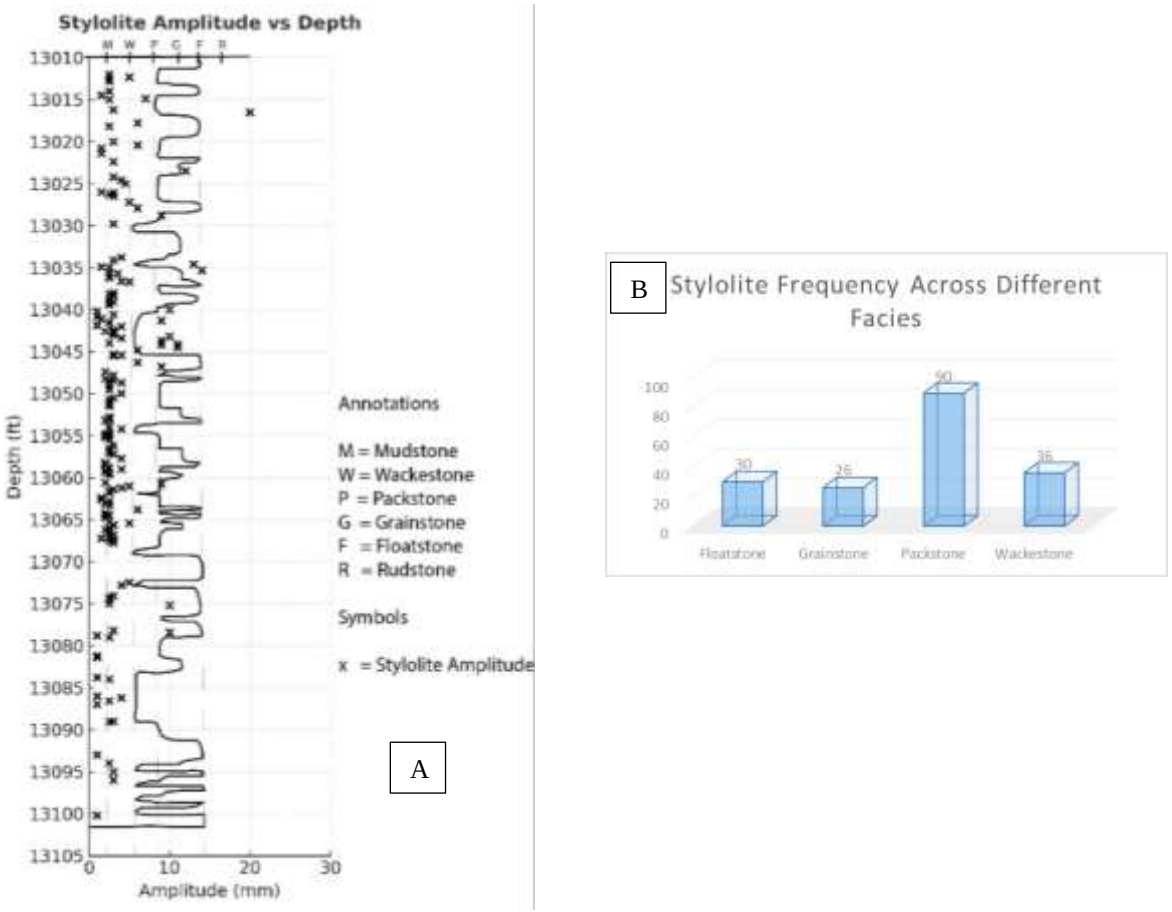

Figure 6. (a) Stylolite distribution in Upper Araej Member. Note that middle section has significant stylolite development. (b) The chart showing the stylolite frequency across different facies. Note that packstone facies has exhibits extensive development of stylolites (n=90)

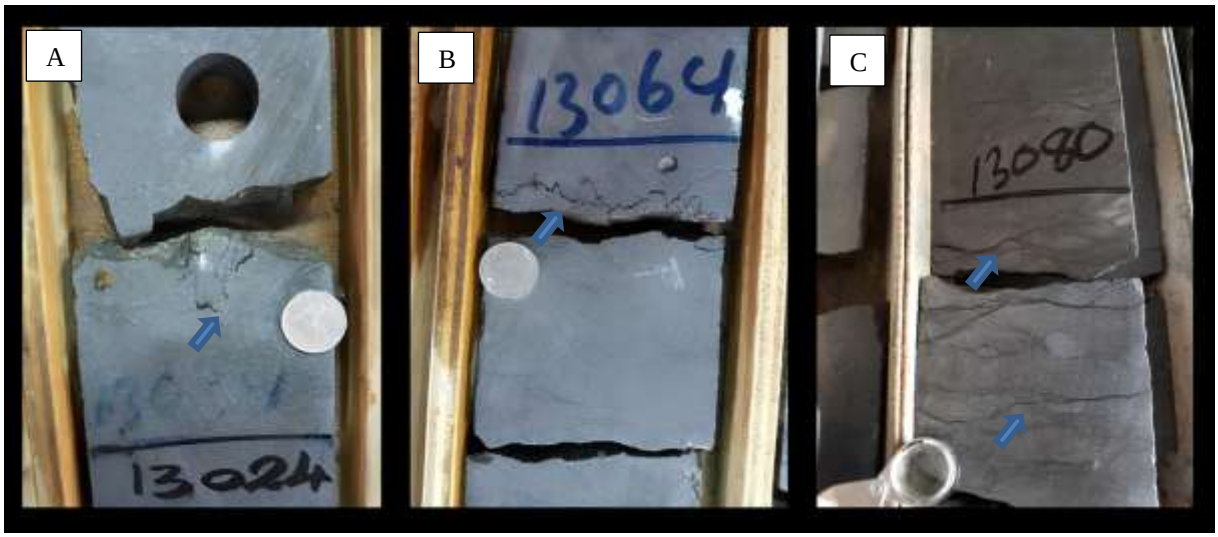

Figure 7. The core photograph showing (a) The occurrence of jagged stylolite in packstone, note that the stylolites are often filled with calcite cement and clay (b) Jagged stylolite in Floatstone (c) Low amplitude stylolite (wispy seams) in mud-dominated packstone.

3.3 Statistical Analysis

The statistical assessment of stylolite amplitude across the principal carbonate facies (Floatstone, Wackestone, Packstone, and Grainstone) yields important insights into facies-dependent diagenetic behavior (Table 1). Descriptive statistics indicate that mean amplitudes are broadly comparable, ranging between 3.0 and 4.1 mm, while median values cluster tightly between 2.5 and 3.0 mm. This convergence suggests that the central tendency of stylolite development is largely insensitive to depositional texture. However, examination of variability and extreme values reveals a more nuanced picture. Floatstones and Grainstones record the largest maximum amplitudes (20 mm and 14 mm, respectively), whereas Packstones and Wackestones rarely exceed 10–13 mm. Such patterns imply that local heterogeneities and stress concentration effects are critical in driving extreme stylolite growth in specific facies.

Table 1. Statistical parameters of stylolite amplitude across different facies

Facies	Mean	Median	Std_Dev	Variance	Min	Max	Count
Floatstone*	4.016667	3	3.541584	12.54282	1	20	30
Grainstone	3.730769	2.5	3.102356	9.624615	1.5	14	26
Packstone*	3.016667	2.5	1.716493	2.946348	1	10	90
Wackestone*	4.097222	2.5	3.32484	11.05456	1	13	36

*mud-rich facies

Boxplot visualization (Figure 8) further underscores these contrasts. Packstones and Grainstones display narrow interquartile ranges, reflecting relatively uniform textural frameworks and more predictable stylolite amplitude. In contrast, Floatstones and Wackestones exhibit broader distributions, consistent with the capacity of mud-supported matrix to facilitate heterogeneous nucleation and irregular propagation. This greater variability in mud-rich facies not only highlights the sensitivity of stylolite development to matrix composition but also underscores their potential to act as permeability barriers and to promote reservoir heterogeneity and anisotropy.

Despite these distinctions in variability, formal hypothesis testing demonstrates no statistically significant differences in stylolite amplitude across facies. One-way ANOVA returned a p value of 0.109, and the non-parametric Kruskal–Wallis test yielded $H = 3.38$ with $p = 0.34$. Both results confirm that amplitude distributions are statistically indistinguishable among facies. Collectively, these findings point to a dual conclusion: while the mean expression of stylolite amplitude is broadly uniform across depositional textures, facies exert a pronounced influence on amplitude variability and extremity.

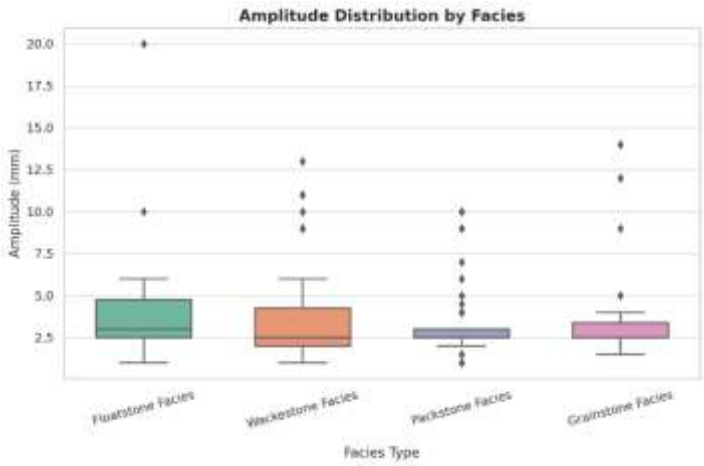

Figure 8. Box plot of stylolite amplitude (vertical offset) across different facies.

3.4 Discussions

Stylolites are a well-known diagenetic feature in carbonate reservoirs, and their development plays an important role in shaping porosity, permeability, and overall reservoir quality. In the onshore Abu Dhabi oil field, our analysis of stylolite amplitudes across different carbonate facies (Floatstone, Wackestone, Packstone, and Grainstone) reveals facies-related tendencies rather than statistically significant differences. Descriptive statistics show that mud-rich facies are generally more prone to stylolite development, with Floatstones and Wackestones yielding higher maximum amplitudes (up to 20 mm and 13 mm, respectively). By contrast, Grainstones exhibit lower average amplitudes, though occasional high-amplitude stylolites (up to 14 mm) are present. These observations suggest that depositional texture influences the variability and extremity of stylolite development, even if mean values are broadly comparable across facies.

Stylolitization in Mud-Rich Facies

The results show that mud-rich facies are most prone to stylolite development. Wackestones and Floatstones yield the highest average amplitudes of stylolite, around 4.1 mm and 4.0 mm respectively, with maximum values reaching 13 mm in wackestones and as much as 20 mm in floatstones. Such high values highlight the sensitivity of these facies to pressure-solution processes. Their fine-grained micritic matrix provides abundant surface area for dissolution, which makes it easier for stylolites to nucleate and propagate during compaction. Stylolite in packstone which dominate the dataset (90 samples) (Figure 6b), have an average amplitude of about 3.0 mm, with values spanning 1 to 10 mm. In this study, packstone are generally mud-dominated packstone (mdp) which implied that high heterogeneity of this facies. Furthermore, this broad spread points to heterogeneous stylolite development, more likely linked to local variations in grain packing, matrix content, and early cementation.

Stylolitization in Grain-Dominated Facies

Grain-dominated facies has less abundant stylolite development. Furthermore, this facies shows low average stylolite amplitudes, even though variability is significant. Grainstones display a slightly higher mean amplitude of 3.7 mm compared to packstone, with some stylolites reaching 14 mm. In some intervals, these stylolites may sharply reduce vertical permeability, creating small-scale barriers or baffles within otherwise high-quality reservoir rock.

Stylolitization, Facies and Reservoir Implications

Jagged stylolites in Upper Araej Member, characterized by sharp peaks and rectangular geometries, are present in both mud-rich and grain-dominated facies, whereas wispy seams are either poorly developed or entirely absent in grainstones. This distribution may suggest that jagged stylolites are controlled primarily by stress concentration along bedding planes and could form regardless of depositional texture, while wispy seams are more strongly associated with micrite-rich facies (e.g. wackstone and packstone). The absence of wispy seams in grainstones possibly reflects the scarcity of clay, which limits the development of diffuse dissolution seams and favors the localization of pressure-solution into discrete, jagged stylolites. Consequently, stylolite morphology in these carbonates provides important insights into the interplay between depositional fabric and diagenetic pressure-solution processes, with implications for reservoir heterogeneity and compartmentalization.

During stylolitization, grains in limestone dissolve at grain-to-grain contacts, and ions migrate by diffusion from zones of dissolution to zones of lower pressure where they precipitate from the solution as intergranular cement [38]. Thus, stylotization can greatly impact on the porosity and permeability.

The considerable amount of carbonate mass, which is expected to be released upon stylolitization of the limestone is commonly assumed to re-precipitate within the succession [39] - [41]. In terms of the occurrence of stylolite in the anticline structure, intensive stylolitization in the flanks would imply a release of larger mass than in the crest [15].

The density of stylolite can be impacted by the lithology with a higher abundance of stylolites in clay-rich limestone [41] [42]. A higher stylolite density was also observed in the clay-rich facies of the Amuri Limestone in the Canterbury Basin by [41]. However, It was reported by [43] that no significant difference in stylolite density was observed between limestone and dolostone within the Khuff Carbonates from offshore Abu Dhabi.

In evaluating the impact of stylolitization on the carbonate reservoir quality, [39] reported that porosity in pelagic carbonates appears nearly absent in thin section analysis; however, core plug measurements indicate porosity values ranging from 5 to 15%, suggesting the presence of microporosity within the micrite matrix. Moreover, studies conducted on compacted chalk buried to a depth of 1 km in the North Sea have shown that it generally retains around 40% porosity, primarily associated with microporosity. It is noteworthy that the chalk described by [39] exhibits significantly lower porosity, which is likely associated with the subsequent effects of stylolite development, particularly the cementation of adjacent micropores.

Our results suggest that stylolite development in this Middle Jurassic Limestone shows facies-related tendencies, though not statistically significant. Mud-supported facies, with their micrite-rich composition, provide favorable conditions for the formation of thicker, more continuous stylolites. Grain-supported facies, by contrast, host more variable and locally controlled stylolite networks. These findings are consistent with earlier work (e.g., [17] [39]), showing that facies architecture plays a central role in diagenetic modification.

In wackestones, packstones and floatstones, stylolites may act as vertical baffles that reduce connectivity and promote reservoir heterogeneity and anisotropy. This might reduce sweep efficiency during secondary recovery. In grainstones, stylolites are less pervasive but still may introduce local anisotropy which baffle fluid flow within the same reservoir unit.

Overall, our findings underscore the complex interplay between facies, lithology, and stylolite development in Jurassic limestones of Upper Araej Member. While micrite-rich, mud-supported facies tend to favor the development of more continuous, high to low amplitude stylolites, the effect of stylolitization on the original microporosity remains unknown. Further investigation using high-resolution techniques, such as scanning electron microscopy (SEM), is recommended to clarify this relationship.

4. Conclussion

This study demonstrates that stylolitization in the Upper Araej Member carbonates of onshore Abu Dhabi exhibits facies-related tendencies. Mud-supported facies, particularly wackestones, floatstones, and mud-dominated packstones, tend to develop thicker and more continuous stylolites, in some cases exceeding 20 mm. Grain-supported facies, especially grainstones, show lower average amplitudes and less pervasive stylolitization, although isolated high-amplitude stylolites (up to 14 mm) can still occur locally and may introduce small-scale flow anisotropy that reduces vertical permeability.

Statistical analysis (ANOVA, $p = 0.109$; Kruskal–Wallis, $H = 3.38$, $p = 0.34$) confirms that these differences are not statistically significant. Nevertheless, descriptive data highlight facies-associated variability and extreme values, suggesting that while average stylolite development is broadly similar across depositional textures, rare but extreme cases in certain facies exert a strong influence on reservoir quality.

Jagged stylolites, which occur in both mud-rich and grain-supported facies, may reflect stress concentration along bedding planes and a relative independence from depositional texture. By contrast, wispy seams are strongly associated with micrite-rich facies (e.g., wackestone and packstone) and are largely absent in grainstones due to the scarcity of clay and fine matrix. This morphological tendency underscores the interplay between depositional fabric and diagenetic pressure-solution processes,

reinforcing the need to consider both stylolite amplitude and morphology when evaluating reservoir heterogeneity.

Reference

[1] Wang, X., Chen, S., Feng, G., Xiao, Z., Yuan, H., Xu, S., & Zhao, H. (2022). Delaminated Fracturing and its Controls on Hydrocarbon Accumulation in Carbonate Reservoirs of Weak Deformation Regions: A Case Study of the Yuanba Ultra-Deep Gas Field in Sichuan Basin, China. *Frontiers in Earth Science*, *10*. https://doi.org/10.3389/feart.2022.884935

[2] Guangyou, Z., Milkov, A., Zhang, Z., Sun, C., Zhou, X., Chen, F., Han, J., & Zhu, Y. (2019). Formation and preservation of a giant petroleum accumulation in superdeep carbonate reservoirs in the southern Halahatang oil field area, Tarim Basin, China. *AAPG Bulletin*, *103*, 1703–1743. https://doi.org/10.1306/11211817132

[3] Fryar, A. E. (2021). Chapter 2 - Groundwater of carbonate aquifers. In A. Mukherjee, B. R. Scanlon, A. Aureli, S. Langan, H. Guo, & A. A. McKenzie (Eds.), *Global Groundwater* (pp. 23–34). Elsevier. https://doi.org/https://doi.org/10.1016/B978-0-12-818172-0.00002-5

[4] Sari, A.S., Bahagiarti, S., Suharsono, S., & Prasetyadi, C. (2020). Groundwater quality in Ponjong Karst, Gunungkidul Regency, Special Region of Yogyakarta. JEMT, 1(1), 7–11.

[5] Rodrigues, H. W. L., Mackay, E. J., & Arnold, D. P. (2022). Multi-objective optimization of CO2 recycling operations for CCUS in pre-salt carbonate reservoirs. *International Journal of Greenhouse Gas Control*, *119*, 103719. https://doi.org/https://doi.org/10.1016/j.ijggc.2022.103719

[6] Hargis, C. W., Chen, I. A., Devenney, M., Fernandez, M. J., Gilliam, R. J., & Thatcher, R. P. (2021). Calcium carbonate cement: A carbon capture, utilization, and storage (ccus) technique. *Materials*, *14*(11). https://doi.org/10.3390/ma14112709

[7] Lv, Q., Zheng, R., Zhou, T., Guo, X., Wang, W., Li, J., & Liu, Z. (2022). Visualization study of CO2-EOR in carbonate reservoirs using 2.5D heterogeneous micromodels for CCUS. *Fuel*, *330*, 125533. https://doi.org/https://doi.org/10.1016/j.fuel.2022.125533

[8] Prahastomi, M., Fahruddin, A., Santy, L. D., & Adlan, R. (2024). Depositional Facies Model and Reservoir Quality of Paleogene Limestone in Labengki Island, Southeast Sulawesi Model Fasies Pengendapan dan Mutu Reservoir Batugamping Paleogen di Pulau Labengki, Sulawesi Tenggara. *Jurnal Geologi Dan Sumberdaya Mineral*, *21*. https://doi.org/10.33332/jgsm.geologi.v23.3.189-196

[9] Ehrenberg, S. N., Morad, S., Yaxin, L., & Chen, R. (2016). Stylolites and porosity in a lower cretaceous limestone reservoir, onshore Abu Dhabi, U.A.E. *Journal of Sedimentary Research*, *86*(10), 1228–1247. https://doi.org/10.2110/jsr.2016.68

[10] Mazzullo, S. J., & Harris, P. M. (2009). *An Overview of Dissolution Porosity Development in the Deep-Burial Environment, With Examples from Carbonate Reservoirs in the Permian Basin*

[11] Deville de Periere, M., Durlet, C., Vennin, E., Caline, B., Boichard, R., & Meyer, A. (2017). Influence of a major exposure surface on the development of microporous micritic limestones - Example of the Upper Mishrif Formation (Cenomanian) of the Middle East. *Sedimentary Geology*, *353*, 96–113. https://doi.org/10.1016/j.sedgeo.2017.03.005

[12] Salindeho, L. M. (2020). Analysis of the relationship between porosity and permeability in reservoir modeling using the petrophysical rock type approach. *Journal of Earth and Marine Technology (JEMT)*, *1*(1), 48–55. https://doi.org/10.31284/j.jemt.2020.v1i1.1188

[13] Koepnick, R. B. (1988). Significance of Stylolite Development in Hydrocarbon Reservoirs with an Emphasis on the Lower Cretaceous of the Middle East. In *Geol. Soc. Malaysia, Bulletin* (Vol. 22).

[14] Morad, D., Nader, F. H., Gasparrini, M., Morad, S., Rossi, C., Marchionda, E., al Darmaki, F., Martines, M., & Hellevang, H. (2018). Comparison of the diagenetic and reservoir quality

evolution between the anticline crest and flank of an Upper Jurassic carbonate gas reservoir, Abu Dhabi, United Arab Emirates. *Sedimentary Geology*, *367*, 96–113. https://doi.org/10.1016/j.sedgeo.2018.02.008

[15] Paganoni, M., al Harthi, A., Morad, D., Morad, S., Ceriani, A., Mansurbeg, H., al Suwaidi, A., Al-Aasm, I. S., Ehrenberg, S. N., & Sirat, M. (2016). Impact of stylolitization on diagenesis of a Lower Cretaceous carbonate reservoir from a giant oilfield, Abu Dhabi, United Arab Emirates. *Sedimentary Geology*, *335*, 70–92. https://doi.org/10.1016/j.sedgeo.2016.02.004

[16] Ehrenberg, S. N., Morad, S., Yaxin, L., & Chen, R. (2016). Stylolites and porosity in a lower cretaceous limestone reservoir, onshore Abu Dhabi, U.A.E. *Journal of Sedimentary Research*, *86*(10), 1228–1247. https://doi.org/10.2110/jsr.2016.68

[17] Railsback, L. (1993). Lithologic controls on morphology of pressure-dissolution surfaces (stylolite and dissolution seams) in Paleozoic carbonate rocks from mideastern United States. *Journal of Sedimentary Research*, 513-522.

[18] Heap, M. J., Baud, P., Reuschlé, T., & Meredith, P. G. (2014). Stylolites in limestones: Barriers to fluid flow? *Geology*, *42*(1), 51–54. https://doi.org/10.1130/G34900.1

[19] Park, W. C., & Schot, E. H. (1968). Stylolites; their nature and origin. *Journal of Sedimentary Research*, *38*(1), 175–191. https://doi.org/10.1306/74D71910-2B21-11D7-8648000102C1865D

[20] Koehn, D., Rood, M. P., Beaudoin, N., Chung, P., Bons, P. D., & Gomez-Rivas, E. (2016). A new stylolite classification scheme to estimate compaction and local permeability variations. *Sedimentary Geology*, *346*, 60–71. https://doi.org/10.1016/j.sedgeo.2016.10.007

[21] Marfil, R., Caja, M. A., Tsige, M., Al-Aasm, I. S., Martín-Crespo, T., & Salas, R. (2005). Carbonate-cemented stylolites and fractures in the Upper Jurassic limestones of the Eastern Iberian Range, Spain: A record of palaeofluids composition and thermal history. *Sedimentary Geology*, *178*(3–4), 237–257. https://doi.org/10.1016/j.sedgeo.2005.05.010

[22] Al-Sharhan, A.S., Salah, M.G.,. (1997). Tectonic implications of diapirism on hydrocarbon accumulation in the United Arab Emirates. *Bulletin of Canadian Petroleum Geology 45*, 279-296.

[23] Glennie, K. W., Boeuf, M.G.A., Clarke, M.W.H., Moody-Stuart, M. . (1973). Late cretaceous nappes in Oman mountains and their geologic evolution. *American Society of Petroleum Geologist Bulletin 57*, 5-27.

[24] Ali, M. Y., Watts, A.B., Searle, M. P. (2013). Seismic stratigraphy and subsidance history of the United Arab Emirates (UAE) rifted margin and overlying forelands basins. *Lithospheric Dynamics and Sedimentary Basins: The Arabian Plate and Analogues*, 127-144.

[25] Boote, D.R.D., Mou, D., Waite, R.I., Robertson, A.H.F., Searle, M.P., Ries, A.C. (1990). Structural evolution of the Sumeinah Forland, central Oman Mountains. *Geological Society Special Publications 49*, 397-418.

[26] Searle, M.P. and Ali M.Y. (2009). Structural and tectonic evolution of the Jabal Sumeini Al Ain-Buraimi region, northern Oman and Eastern United arab Emirates. *GeoArabia 14*, 115-142.

[27] Agard, P., Omrani, J., Jolivet, L., Mouthereau, F.,. (2005). Convergence history across Zagros (Iran): constraints from collisional and earlier deformation. *International Journal of Earth Science*, 401-419.

[28] Agard, P., Omrani, J., Jolivet, L., Whitechurch, H., Vrielynck, B., Spakman, W., Monie, P., Meyer, B., Wortel, R.,. (2011). Zagros orogeny: a subduction dominated process. *Geological Magazine 148*, 692-725.

[29] Imlay, R. (1970). Some Jurassic ammonites from central Saudi Arabia. *US Geological Survey Professional Paper*, G4BD.

[30] Alsharhan, A. S., & Whittle, G. L. (1995). Sedimentary-diagenetic interpretation and reservoir characteristics of the Middle Jurassic (Araej Formation) in the southern Arabian Gulf. In *Petroleum Geology* (Vol. 12, Issue 6).

[31] De Matos, J. E. (2002). Sequence stratigraphy and sedimentation of the Araej Formation (Middle Jurassic), UAE: outcrop and subsurface. *Abu Dhabi International Petroleum Exhibition & Conference.* Abu Dhabi: Society of Petroleum Engineer.

[32] Morad, S., Al-Aasm, I. S., Nader, F. H., Ceriani, A., Gasparrini, M., & Mansurbeg, H. (2012). Impact of diagenesis on the spatial and temporal distribution of reservoir quality in the Jurassic Arab D and C members, offshore Abu Dhabi oilfield, United Arab Emirates. *GeoArabia*, *17*(3), 17–56. https://doi.org/10.2113/geoarabia170317

[33] Grötsch, J., Suwaina, O., Ajlani, G., Taher, A., El-Khassawneh, R., Lokier, S., & Dorp, J. V. (2003). The Arab Formation in central Abu Dhabi: 3-D reservoir architecture and static and dynamic modeling. GeoArabia, 8(1), 47-86.

[34] Embry, A. F., & Klovan, J. E. (1971). A late Devonian reef tract on Northern Banks Island. *Bulletin of Canadian Petroleum Geology*, *19*(4), 730–781. https://doi.org/10.35767/gscpgbull.19.4.730

[35] Lucia, F. J. (1995). Rock-Fabric/Petrophysical Classification of Carbonate Pore Space for Reservoir Characterization1. *AAPG Bulletin*, *79*(9), 1275–1300. https://doi.org/10.1306/7834D4A4-1721-11D7-8645000102C1865D

[36] Fisher, R. A. (1992). Statistical Methods for Research Workers. In N. L. Kotz Samuel and Johnson (Ed.), *Breakthroughs in Statistics: Methodology and Distribution* (pp. 66–70). Springer New York. https://doi.org/10.1007/978-1-4612-4380-9_6

[37] Gibbons, J.D., & Chakraborti, S. (2020). Nonparametric Statistical Inference (6th ed.). Chapman and Hall/CRC. https://doi.org/10.1201/9781315110479

[38] Drummond, C.N., Sexton, D.N., 1998, Fractal structure of stylolites: Journal of Sedimentary Research, v. 68, p. 8–10.

[39] Oswald, E. J., Mueller III, H. W., & Goff, D. F. (1995). Controls on porosity evolution in Thamama Group carbonate reservoirs in Abu Dhabi, UAE. *Society of Petroleum Engineer*.

[40] Fabricus, I. D. A. L., & Borre, M. A. I. K. (2007). Stylolites, porosity, depositional texture, and silicates in chalk facies sediments. Ontong Java Plateau – Gorm and Tyra fields, North Sea. *Sedimentology*, *54*(1), 183–205. https://doi.org/https://doi.org/10.1111/j.1365-3091.2006.00828.x

[41] Vandeginste, V., & John, C. M. (2013). Diagenetic implications of stylolitization in pelagic carbonates, Canterbury Basin, offshore New Zealand. *Journal of Sedimentary Research*, *83*(3), 226–240. https://doi.org/10.2110/jsr.2013.18

[42] Oldershaw, A.E., Scoffin, T. P., 1967, The source of ferroan and non-ferroan calcite cements in the Halkin and Wenlock Limestones: Geological Journal, v. 5, p. 309–320.

[43] Peacock, D. C. P., & Azzam, I. N. (2006). Development and scaling relationships of a stylolite population. *Journal of Structural Geology*, *28*(10), 1883–1889. https://doi.org/https://doi.org/10.1016/j.jsg.2006.04.008